Received: 2 April 2020 | Revised: 12 June 2020 | Accepted: 1 July 2020

DOI: 10.1002/elsc.202000024

Engineering in Life Sciences

RESEARCH ARTICLE

Performance evaluation of a high-throughput separation system for circulating tumor cells based on microcavity array

Ryo Negishi | **Hyuga Saito** | **Reito Iwata** | **Tsuyoshi Tanaka** | **Tomoko Yoshino**

Division of Biotechnology and Life Science, Institute of Engineering, Tokyo University of Agriculture and Technology, Tokyo, Japan

Correspondence
Tomoko Yoshino, Division of Biotechnology and Life Science, Institute of Engineering, Tokyo University of Agriculture and Technology, 2-24-16, Naka-cho, Koganei, Tokyo 184–8588, Japan.
Email: y-tomoko@cc.tuat.ac.jp

Funding information
Japan Science and Technology Agency, Grant/Award Number: JPMJMI18G9; Core Research for Evolutional Science and Technology, Grant/Award Number: JPMJCR14G5

Abstract

Circulating tumor cells (CTCs) are widely known as useful biomarkers in the liquid biopsies of cancer patients. Although single-cell genetic analysis of CTCs is a promising diagnostic tool that can provide detailed clinical information for precision medicine, the capacity of single-CTC isolation for genetic analysis requires improvement. To overcome this problem, we previously developed a multiple single-cell encapsulation system for CTCs using hydrogel-encapsulation, which allowed for the high-throughput isolation of single CTCs. However, isolation of a single cell from adjacent cells remained difficult and often resulted in contamination by neighboring cells due to the limited resolution of the generated hydrogel. We developed a novel multiple single-cell encapsulation system equipped with a high magnification lens for high throughput and a more accurate single-cell encapsulation. The multiple single-cell encapsulation system has sufficient sensitivity to detect immune-stained CTCs, and could also generate a micro-scaled hydrogel that can isolate a single cell from adjacent cells within 10 μm, with high efficiency. The proposed system enables high throughput and accurate single-cell manipulation and genome amplification without contamination from neighboring cells.

KEYWORDS

circulating tumor cells (CTCs), photopolymerizable hydrogel, single-cell analysis, whole genome amplification

1 | INTRODUCTION

Circulating tumor cells (CTCs) are rare metastatic cancer cells derived from the primary tissue that circulate in the bloodstream [1, 2]. CTC-based liquid biopsy is recognized as a useful biomarker for cancer diagnoses. Genetic analyses of single CTCs provide critical insights into

Abbreviations: CTCs, circulating tumor cells; DMD, digital micromirror device; MCA, microcavity array; PEGDA, Poly(ethylene glycol)-diacrylate

cancer metastases and add detailed clinical information that enhances patient care [3–5]. The recovery of CTCs from blood has mainly involved immunoseparation- or physical-based approaches. Immunomagnetic separation with tumor cell markers is commonly used for CTC recovery [6–10]. Immunoseparation-based approaches are limited in application to various types of tumor cells because the expression level of the target antigen varies among tumor types [11–13]. Physical-based approaches, such as microfilters, microfluidic devices or dielectrophoresis, have been applied to various types of CTCs that cannot be detected with immunoseparation-based recovery methods [14–18]. Although these technologies allow for the efficient recovery of a single CTC, the throughput of single-CTC isolation for subsequent genetic analyses remains low [4, 19–21]. Therefore, a high-throughput technology for the manipulation of single cells is required for the advanced application of CTCs in liquid biopsy.

To enable high throughput manipulation of CTCs, we employed a physical-based CTC recovery from whole blood using a microcavity array (MCA), which demonstrated highly efficient recovery of cancer cells based on differences in cell size and deformability [22–24]. Our recent studies have indicated that an MCA with a rectangular pore could improve the recovery efficiency of small-sized cancer cells and reduce contamination with leukocytes [25]. Cancer cells captured on the MCA can be encapsulated by a hydrogel for subsequent genetic analyses of single CTCs [26]. The multiple single-cell encapsulation system was developed for the high-throughput manipulation of CTCs through the integration of wide-field fluorescence imaging and hydrogel photo-polymerization systems with a digital micromirror device (DMD) [27]. The multiple single-cell encapsulation system integrated with these technologies allows for the high throughput hydrogel-encapsulation of single cells by parallel control of light irradiation. However, it was impossible to separate a target cell from adjacent cells entrapped on the rectangular microcavities due to limited resolution of the generated hydrogel. To further improve the performance of the multiple single-cell encapsulation system, the area of the hydrogel reserved for the target cell on the MCA was minimized for single-cell manipulation to avoid contamination of the target cell by neighboring cells.

In this study, a novel multiple single-cell encapsulation system with high magnification objective lenses was constructed for high throughput and more accurate encapsulation of single cells. To evaluate the performance of the new system, the sensitivity of the wide-field fluorescence imaging system was compared with conventional fluorescence microscopy. The photopolymerization conditions for single-cell encapsulation were optimized.

PRACTICAL APPLICATION

Single-cell genetic analysis of circulating tumor cells (CTCs) has great potential for use as a minimally invasive diagnostic tool. However, the number of CTCs in peripheral blood is extremely low, and the high throughput manipulation of CTCs remains a technical challenge. In this study, we developed a multiple single-cell encapsulation system, which allows for the detection and isolation of single CTCs from blood. The newly designed optical system provides sufficient sensitivity for the detection of immuno-stained CTCs, and a micro-scaled hydrogel that allows for the isolation of a single cell from adjacent cells located within 10 μm, was generated. The isolated single cells could be used for whole genome amplification with sufficient quality for single-cell genetic analyses. This study demonstrates the great potential of this new system for use in CTC-based liquid biopsy.

2 | MATERIALS AND METHODS

2.1 | Construction of the multiple single-cell encapsulation system

Figure 1 shows a schematic diagram of the multiple single-cell encapsulation system developed in this study. The system comprised two optical systems: a wide-field fluorescence imaging system (Figure 1A) and a photopolymerization system for single-cell encapsulation (Figure 1B). The light path was identical in both systems and was controlled by DMD, DLP7000UV; 1024 × 768 pixels with a pixel size of 13.6 × 13.6 μm^2; Texas Instruments, Dallas, TX, USA; Figure 1A-c, 1B-c), which simplified the optical system.

The wide-field fluorescence imaging system was designed to visualize 2D fluorescence imaging in an area of 12.1 × 8.6 mm^2 for a 2x objective lens, 2.5 × 1.2 mm^2 for a 10x objective lens, and 0.59 × 0.52 mm^2 for a 40x objective lens. Fluorescence images of the entire MCA (6.0 × 6.0 mm^2) were captured using a CMOS sensor (Figure 1A-j, B-j) with 2x and 10x objective lenses, and detailed morphological analyses were performed with a 40x objective lens (Figure 1A-g, 1B-g). Band path filters and dichroic mirrors used are summarized in Table S1. Performance of the fluorescence imaging system was evaluated using a calibration slide for the microarray scanner (DS01; Full Moon Biosystems, CA, USA), and compared with a fluorescence microscope (BX53; Olympus Corporation,

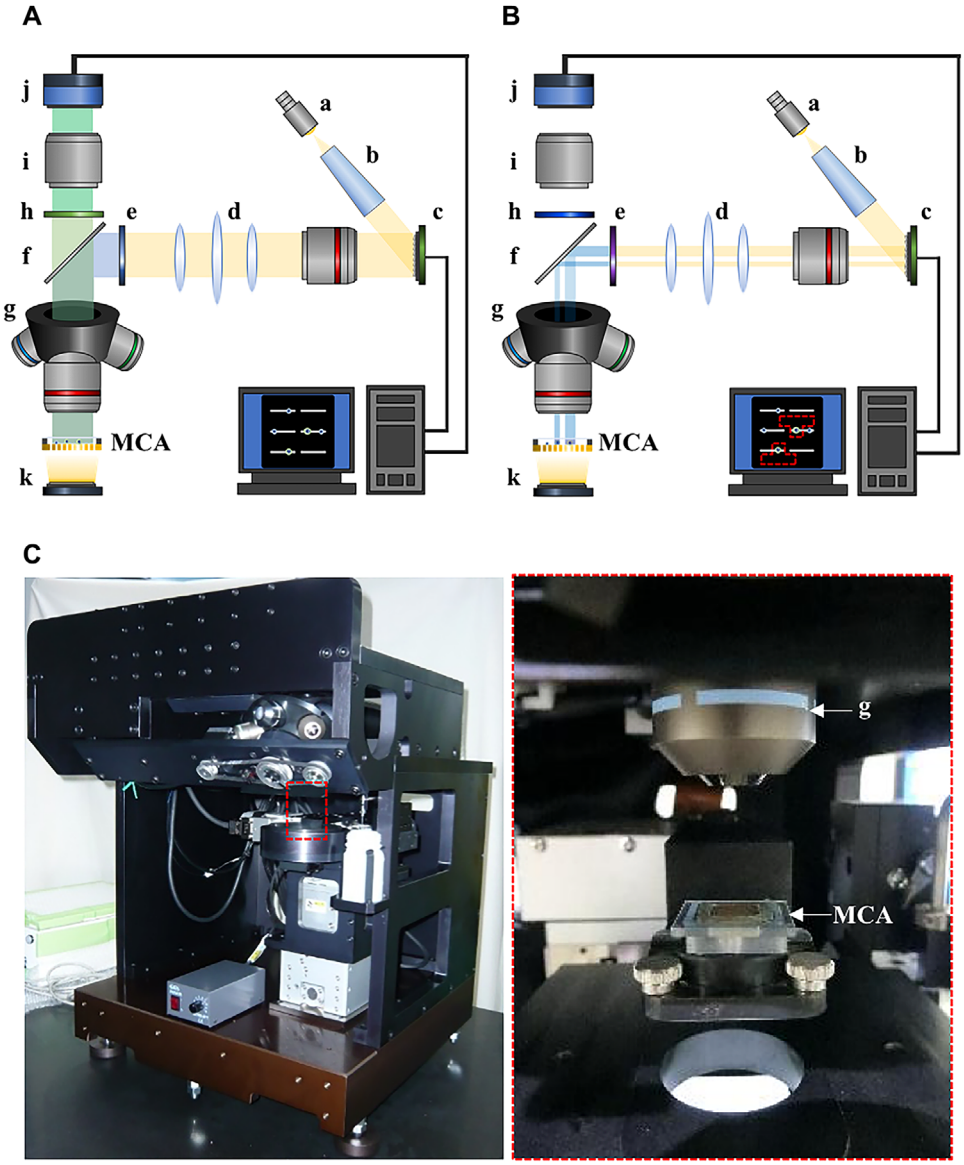

FIGURE 1 Schematic diagram of the multiple single-cell encapsulation system, comprising (A) the wide-field fluorescence imaging system and (B) the photopolymerization system. (C) Overview of the integrated system. a: Light source, b: Tapered light pipe homogenizing rods, c: DMD, d: Relay lenses, e: Excitation filter, f: Dichroic mirror, g: Objective lenses, h: Emission filter, i: format fixed focal length lenses, j: CMOS sensor, k: LED light

Tokyo, Japan) equipped with a cooled digital camera (ExiAqua; QImaging, BC, Canada).

The photopolymerization system for single-cell encapsulation was controlled by the DMD. The curing light (λ_{max} = 365 nm) modulated by the DMD was projected onto an MCA after passing through each filter (Table S1) for hydrogel generation. Generated hydrogels were observed using an SEM (VE-9800; Keyence Corp., Osaka, Japan) after gold-coating by sputtering using an E-1010 ion sputter (Hitachi, Ltd., Tokyo, Japan). Figure 1C shows the entire system; the two optical systems were integrated.

2.2 | Cancer cell samples

Two cancer cell lines with different sizes, NCI-H1975 (ATCC CRL5908) and NCI-N87 (ATCC CRL5822), were used in this study. Cell lines were cultured in RPMI 1640 medium as described previously [28]. Immediately prior to each experiment, cells grown to confluence were trypsinized, and stained with 5 μM CellTracker Green CMFDA (5-chloromethylfluorescein diacetate; Thermo Fisher Scientific, Waltham, MA, USA) for 30 min, and centrifuged at 400 × *g* for 3 min to obtain cell pellets. After

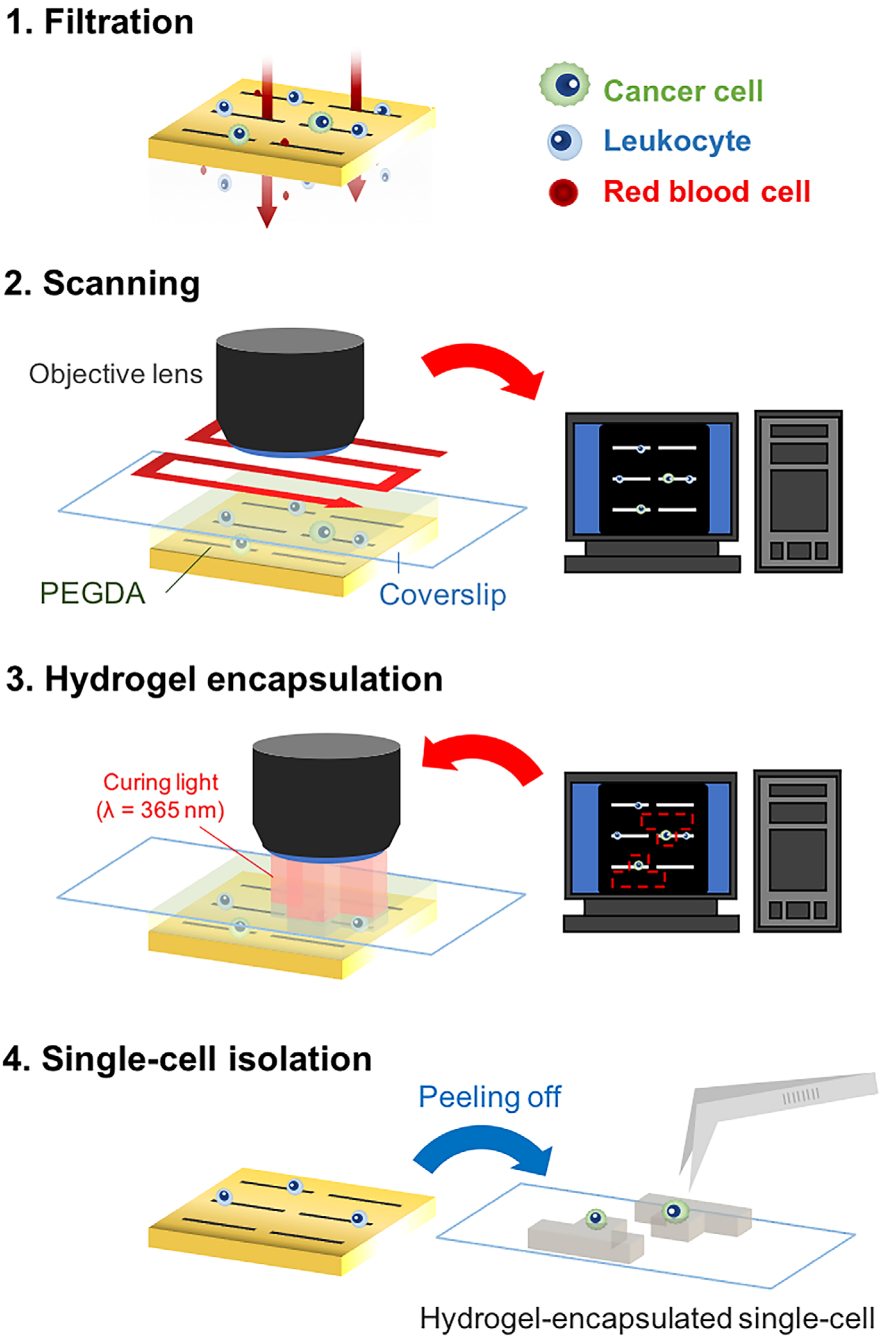

FIGURE 2 Experimental procedure for single-cell isolation using the multiple single-cell encapsulation system

washing twice with PBS, the cells were re-suspended in PBS with 0.5% BSA and 2 mM EDTA. The sample (1 mL) was passed through the MCA at a flow rate of 200 μL/min for 5 min. A flow rate of filtration was optimized by cancer cell recovery tests in previous report [22]. An MCA with a rectangular pore (8 μm × 100 μm, 6.7% porosity) (Hitachi Chemical Co., Ltd., Tokyo, Japan) was used (Figure S1). MCAs were fabricated by electroplating method and integrated with PDMS-made microfuidic device described in previous reports [23, 25].

The cancer cell line, NCI-N87 (1×10^3 cells) spiked into human blood (1 mL) was prepared as a model CTC sample. After cell assembly on the MCA, entrapped cells were fixed with paraformaldehyde and permeabilized with Triton-X-100 by introducing each reagent for 15 min, respectively. To distinguish cancer cells from leukocytes, the cells entrapped on the MCA were stained with AlexaFluor 488-labeled anti-cytokeratin and TexasRed-labeled anti-CD45 antibodies (Hitachi Chemical Co., Ltd., Japan) for 30 min. The concentration of paraformaldehyde, Triton-X-100 and

flurorescence-labeled antibodies were previously optimized [23, 25]. Human blood samples were collected from healthy donors at the Tokyo University of Agriculture and Technology. Experimental protocols were approved by the Institutional Review Board of the Tokyo University of Agriculture and Technology (Approval code: No. 30-10).

2.3 | Hydrogel-encapsulation of CTCs

The procedure for the hydrogel encapsulation of single cells is shown in Figure 2. Poly(ethylene glycol)-diacrylate (PEGDA) prepolymer (number-average molecular weight [Mn] = 700 Da; Sigma-Aldrich, MO, USA) and Irgacure 2959 (1-[4-(2-hydroxyethoxy)-phenyl]-2-hydroxy-2-methyl-1-propane-1-one; Sigma-Aldrich, MO, USA) were used as photoinitiators. PEGDA prepolymer with 0.3% Irgacure 2959 was introduced onto single cells entrapped on the MCA. The sample was mounted onto the multiple single-cell encapsulation system and subjected to image acquisition and light irradiation. Fluorescence images were captured using the CMOS sensor (Figure 2). Targeted single cells were exposed to the curing light ($\lambda_{max} = 365$ nm), and single cells were encapsulated by the generated PEGDA hydrogel (Figures 2 (3)). Hydrogel encapsulated single cells were collected by coverslip peeling from the MCA (Figures 2 (4)); the surface of the coverslip was coated prior to peeling with 3-(trimethoxysilyl)propyl methacrylate covalently bound to PEGDA hydrogels. Each hydrogel was transferred to a 200 μL PCR tube using tweezers for subsequent whole genome amplification (WGA) reactions.

2.4 | Whole genome amplification of single cells

Hydrogel encapsulated single cells were subjected to WGA using the Ampli1 WGA kit (Silicon Biosystems, Bologna, Italy), according to the manufacturer's protocol. As a control, single cells isolated by a micromanipulator (PicoPipet; Nepagene, Chiba, Japan) were also subjected to WGA. WGA products were purified using the MinElute PCR Purification kit (Qiagen, Hilden, Germany). The final concentration of WGA products was determined using Quant-iT PicoGreen dsDNA Assay Kit (Thermo Fisher Scientific, Waltham, MA, USA). To measure the integrity of the WGA products, a multiplex PCR of four fragments of differing lengths from different chromosomes (chromosome 12p, 91 bp; chromosome 5q, 108–166 bp; chromosome 17p, 299 bp; chromosome 6q, 614 bp) was performed using the Ampli1 QC kit (Silicon Biosystems, Bologna, Italy). PCR amplicons were visualized using the Agilent DNA 1000 kit (Agilent Biotechnology, Santa Clara, CA, USA).

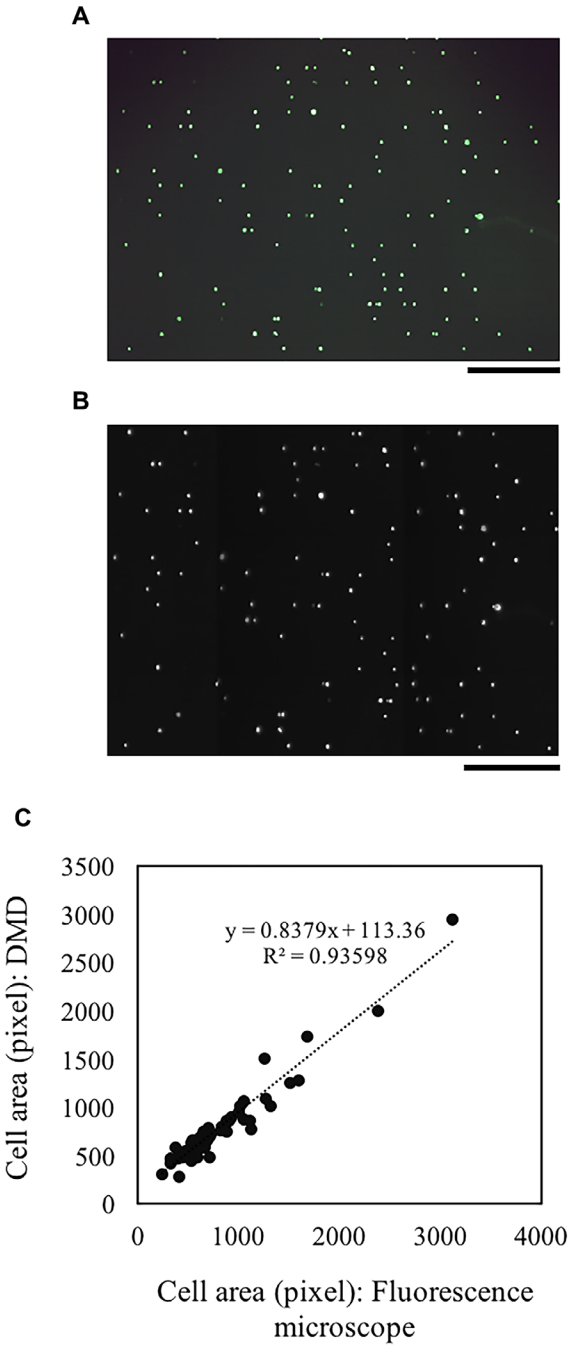

FIGURE 3 Fluorescence images of immuno-stained NCI-H1975 cells, obtained by the wide-field fluorescence imaging system (A), and fluorescence microscopy (B). Scale bar: 500 μm. (C) Correlation of cell area for each single cell between the wide-field fluorescence imaging system and the fluorescence microscope

3 | RESULTS AND DISCUSSION

3.1 | Performance evaluation of the wide-field fluorescence imaging system

Prior to evaluation of single-cell isolation, LOD of the wide-field fluorescence imaging system that was

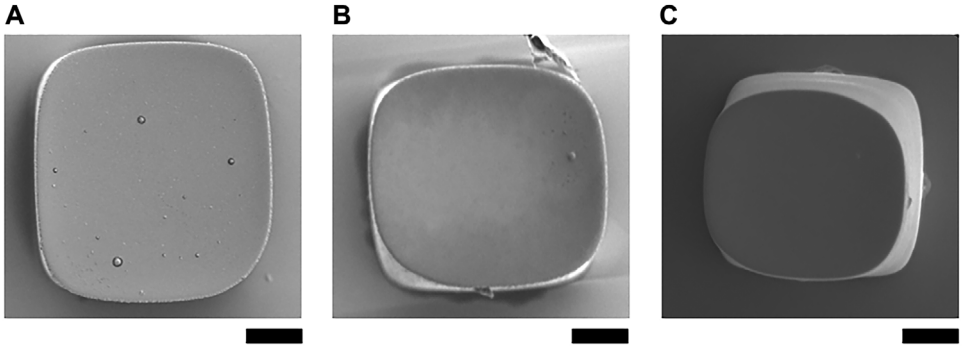

FIGURE 4 SEM images of hydrogel generated by the multiple single-cell encapsulation system. Scale bar = 50 μm. (A) 3.3×10^2 mW/cm^2 for 30 s. (B) 1.3×10^2 mW/cm^2 for 77 s. (C) 0.6×10^2 mW/cm^2 for 165 s

integrated in the multiple single-cell encapsulation system was calculated to compare with conventional fluorescence microscopy. The LOD was determined through visualization of a calibration slide with Cy3 spots in a dilution series (Figure S2A) and was defined as the minimum detectable signal for which the signal-to-noise ratio was more than 3. The LOD of the wide-field fluorescence imaging system was 2.1×10^2 molecules-Cy3/μm^2 (Figure S2B), which was identical to the level obtained with the fluorescence microscope (1.0×10^2 molecules-Cy3/μm^2; Figure S2C, D). As the expression of cellular marker proteins, such as cytokeratin, was estimated to be approximately 10^5 molecules/cells, i.e. 1.3×10^3 molecules/μm^2 (cell diameter = 10 μm), the proposed system was predicted to have sufficient sensitivity to detect CTCs [29, 30]. To confirm this sensitivity, cancer cells with immuno-stained cytokeratin, were visualized by the new system. Figure 3A shows fluorescence images of immuno-stained NCI-H1975 cells entrapped on the MCA by the wide-field fluorescence imaging system. Individual cells were successfully visualized as same as the fluorescence microscope (Figure 3B). The cell sizes visualized by the wide-field fluorescence imaging system were appropriate for microscopy-based evaluation (Figure 3C); the new system maintained sufficient sensitivity to detect and visualize CTCs.

3.2 | Determination of photopolymerization conditions for single-cell encapsulation

The relationship between fluence rate (mW/cm^2) and exposure time (s) in hydrogel photopolymerization was investigated to optimize the conditions for use of the multiple single-cell encapsulation system with a 10x objective lens. The irradiation light fluence was fixed at 10 J/cm^2. Three conditions (1) high-light (3.3×10^2 mW/cm^2) and short-exposure time (30 s), (2) medium-light (1.3×10^2 mW/cm^2) and medium-exposure time (77 s) and (3) low-light (0.6×10^2 mW/cm^2) and long-exposure time (165 s) were examined for comparison. A square pattern (200 μm × 200 μm) of light was projected to a coverslip with a hydrogel precursor using the multiple light irradiation system. The predicted size of hydrogel was generated in only condition 1; however, other conditions 2 and 3 resulted in smaller-sized hydrogels (Figure 4). These results indicate that the photopolymerization for cell encapsulation was most affected by fluence rate (mW/cm^2) during the tested conditions. The high-light condition, the light fluence of 6.5–6.6 J/cm^2 was sufficient to generate the necessary hydrogels size (200 μm × 200 μm square). Therefore, the photopolymerization conditions were fixed at the fluence of 6.5 J/cm^2 in subsequent experiments.

3.3 | Investigation of single-cell isolation by hydrogel encapsulation

Single-cell isolation by hydrogel-photopolymerization was examined at the optimized conditions as mentioned previously. In this experiment, a convex-type hydrogel was generated for single-cell isolation using a 40x objective lens (Figure 5A). Prior to single-cell isolation experiments, we evaluated cancer cell recovery efficiency of the rectangular MCA. The recovery efficiency of spiked NCI-H1975 cells was more than 95% that is comparable with the current systems [24,31]. Figure 5B shows a typical image of two adjacent cancer cells (NCI-H1975) entrapped on the rectangular MCA. In this experiment, one cell was separated from other cells at a distance of approximately 10 μm. When a convex pattern of light, indicated by a red dotted line, was projected on to the surface (Figure 5A,B), a single cell was successfully isolated from the adjacent cells using the protrusion part of the convex-type hydrogel

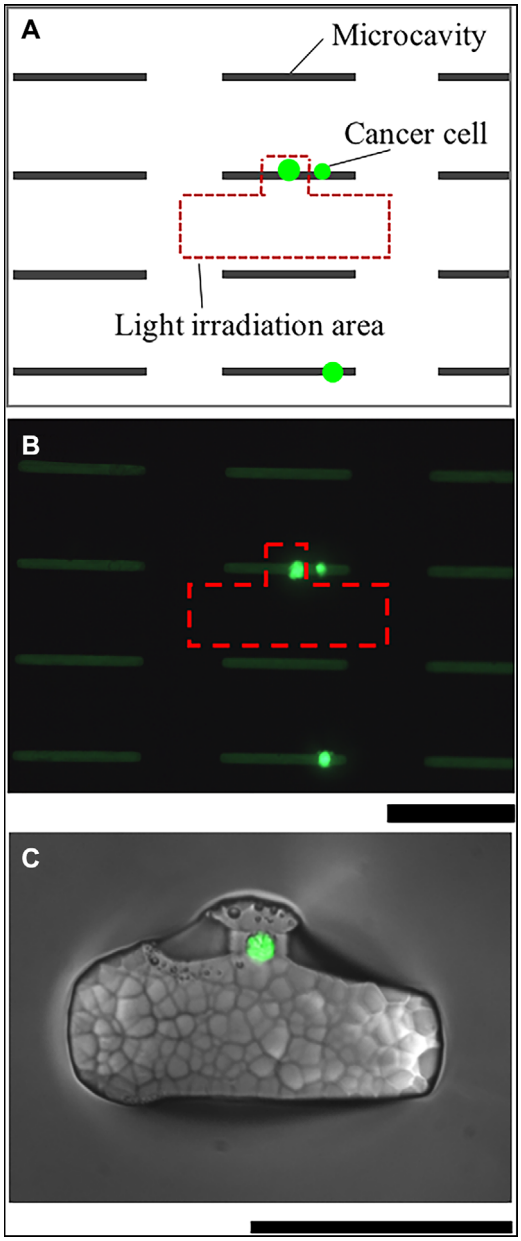

FIGURE 5 (A) Schematic of cancer cells entrapped on the microcavity array (MCA). (B) Fluorescence image of CellTracker Green stained NCI-H1975 cells on the MCA. The target cell was encapsulated onto a convex-type hydrogel. Scale bar: 100 μm. (C) Merged bright field and fluorescence image of a convex-type hydrogel recovered from MCA. Scale bar: 100 μm

(Figure 5C). These results indicate that the convex-type hydrogel allows for accurate separation of single cells from adjacent cells on the rectangular MCA, without contamination from cells in neighboring microcavities.

Single-cell isolation with two cell lines of different sizes was performed to compare isolation efficiency between cell types. A human lung adenocarcinoma cell line, NCI-H1975 (cell diameter: 23.5 ± 6.4 μm) and a human gastric carcinoma cell line, NCI-N87 (cell diameter: 12.2 ± 1.4 μm)

TABLE 1 Quality of whole genome amplification products obtained from isolated single NCI-N87 cells

Sample	Rates of good quality DNA[a]
Hydrogel-encapsulated single cells	75.0% (n = 16 cells)
Non-photopolymerized cells (control)	72.7% (n = 22 cells)

[a]The quality was evaluated by a multiplex PCR-base method, and three or four PCR bands were defined as good quality DNA.

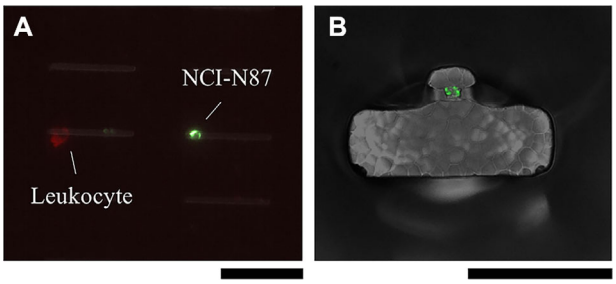

FIGURE 6 (A) Fluorescence image of a cancer cell and a leukocyte entrapped on the microcavity array (MCA) from a blood sample using the multiple single-cell encapsulation system. (B) Image of hydrogel-encapsulated cancer cell isolated from the MCA (B). Scale bar: 100 μm

were used. Highly efficient cell isolation was accomplished using the convex-type hydrogel; identical isolation was achieved with both cell sizes. The cell isolation rates were 97.6% (41/42) for NCI-H1975 cells and 94.4% (51/54) for NCI-N87. These values were nearly identical to previous studies using confocal laser scanning microscopy [26].

To evaluate the effect of photopolymerization on genetic analysis, WGA was carried out using hydrogel-encapsulated single cells. Sufficient DNA (1.06 ± 0.52 μg per cell) was successfully obtained by WGA, however, there was a lower yield of WGA products than non-photopolymerized cells (1.58 ± 0.51 μg per cell). WGA could be partially hindered in the presence of a hydrogel. The quality of WGA products was verified by a multiplex PCR-based method using Ampli1 QC kit which produces three or four PCR bands from single cells with good quality DNA. Most single cells (75%) provided a good quality of DNA with more than three bands, which was identical to the control (Table 1). These results indicate that the DNA quality of WGA products obtained by the proposed method was adequate for single-cell genomic analyses.

Single-cell isolation was also examined using whole blood spiked with NCI-N87 cells. Figure 6 shows fluorescence image of a cancer cell and a leukocyte enriched from whole blood by MCA. Cells positively stained for the nucleus and cytokeratin, and negative for CD45 were scored as cancer cells; cells stained positive for the nucleus

and CD45, and negative for cytokeratin were scored as leukocytes. Only a single cancer cell was successfully isolated from MCA using the protrusion part of convex-type hydrogel (Figure 6B). These results indicate that the proposed system can be applied to whole blood samples. The multiple single-cell encapsulation system allows for the encapsulation of 15 CTCs in parallel within 3 s, indicating high throughput and accurate single-cell manipulation and genome amplification can be achieved without contamination of the target cell with neighboring cells.

4 | CONCLUDING REMARKS

In this study, we developed a novel multiple single-cell encapsulation system controlled by a DMD and equipped with a series of objective lenses. The system comprised wide-field fluorescence imaging and photopolymerization systems for single-cell encapsulation. Fluorescence imaging in an area of MCA was rapidly observed with sufficient sensitivity to detect fluorescent antibody-labeled CTCs using the wide-field fluorescence imaging system. Furthermore, the relationship between the fluence rate and the exposure time in hydrogel photopolymerization was investigated, and the high-light condition (fluence: 6.5 J/cm^2) was determined to be optimal.

Convex-type hydrogels enable the isolation of a desired single cell from adjacent cells on the rectangular MCA with high rate of isolation (>94%). Light irradiation and photopolymerizaion did not affect the quality of the amplified WGA products for single-cell genomic analyses. Our proposed system provides an attractive application for other targets such as adherent cells, tissue samples, and microorganisms, in addition to widespread use in the isolation of CTCs for liquid biopsy.

ACKNOWLEDGEMENT

This work was supported by JST, CREST (JPMJCR14G5), and JST-Mirai Program Grant Number JPMJMI18G9, Japan.

CONFLICT OF INTEREST

The authors have declared no conflict of interest.

REFERENCES

1. Vona, G., Sabile, A., Louha, M., Sitruk, V., et al. Isolation by size of epithelial tumor cells : A new method for the immunomorphological and molecular characterization of circulatingtumor cells. Am. J. Pathol. 2000, 156, 57–63.
2. Cristofanilli, M., Budd, G. T., Ellis, M. J., Stopeck, A., et al. Circulating tumor cells, disease progression, and survival in metastatic breast cancer. N. Engl. J. Med. 2004, 351, 781–791.
3. Carter, L., Rothwell, D. G., Mesquita, B., Smowton, C., et al. Molecular analysis of circulating tumor cells identifies distinct copy-number profiles in patients with chemosensitive and chemorefractory small-cell lung cancer. Nat. Med. 2017, 23, 114–119. PMID:27869802
4. Gkountela, S., Castro-Giner, F., Szczerba, B. M., Vetter, M., et al. Circulating tumor cell clustering shapes DNA methylation to enable metastasis seeding. Cell 2019, 176, 98–112.e114.
5. Miyamoto, D. T., Zheng, Y., Wittner, B. S., Lee, R. J., et al. RNA-Seq of single prostate CTCs implicates noncanonical Wnt signaling in antiandrogen resistance. Science 2015, 349, 1351–1356.
6. Allard, W. J., Matera, J., Miller, M. C., Repollet, M., et al. Tumor cells circulate in the peripheral blood of all major carcinomas but not in healthy subjects or patients with nonmalignant diseases. Clin. Cancer Res. 2004, 10, 6897–6904.
7. Nagrath, S., Sequist, L. V., Maheswaran, S., Bell, D. W., et al. Isolation of rare circulating tumour cells in cancer patients by microchip technology. Nature 2007, 450, 1235–1239.
8. Sun, Y., Chen, Y., Li, S., Lei, Y., et al. NanoVelcro-captured CTC number concomitant with enhanced serum levels of MMP7 and MMP9 enables accurate prediction of metastasis and poor prognosis in patients with lung adenocarcinoma. Int J Nanomedicine 2017, 12, 6399–6412.
9. Lee, S.-W., Hyun, K.-A., Kim, S.-I., Kang, J.-Y., et al. Enrichment of circulating tumor cells using a centrifugal affinity plate system. J. Chromatogr. A 2014, 1373, 25–30.
10. Zhao, L., Tang, C., Xu, L., Zhang, Z., et al. Enhanced and differential capture of circulating tumor cells from lung cancer patients by microfluidic assays using Aptamer Cocktail. Small 2016, 12, 1072–1081.
11. Mayer, J. A., Pham, T., Wong, K. L., Scoggin, J., et al. FISH-based determination of HER2 status in circulating tumor cells isolated with the microfluidic CEE platform. Cancer Genet. 2011, 204, 589–595.
12. Lin, H. C., Hsu, H. C., Hsieh, C. H., Wang, H. M., et al. A negative selection system PowerMag for effective leukocyte depletion and enhanced detection of EpCAM positive and negative circulating tumor cells. Clin. Chim. Acta 2013, 419, 77–84.
13. Ozkumur, E., Shah, A. M., Ciciliano, J. C., Emmink, B. L., et al. Inertial focusing for tumor antigen-dependent and -independent sorting of rare circulating tumor cells. Sci. Transl. Med. 2013, 5, 179ra147.
14. Farace, F., Massard, C., Vimond, N., Drusch, F., et al. A direct comparison of CellSearch and ISET for circulating tumour-cell detection in patients with metastatic carcinomas. Br. J. Cancer 2011, 105, 847–853.
15. van der Toom, E. E., Groot, V. P., Glavaris, S. A., Gemenetzis, G., et al. Analogous detection of circulating tumor cells using the AccuCyte((R)) -CyteFinder((R)) system and ISET system in patients with locally advanced and metastatic prostate cancer. Prostate 2018, 78, 300–307.
16. Mazzini, C., Pinzani, P., Salvianti, F., Scatena, C., et al. Circulating tumor cells detection and counting in uveal melanomas by a filtration-based method. Cancers 2014, 6, 323–332.
17. Kim, Y. J., Kang, Y. T., Cho, Y. H., Poly(ethylene glycol)-modified tapered-slit membrane filter for efficient release of captured viable circulating tumor cells. Anal. Chem. 2016, 88, 7938–7945.

18. Warkiani, M. E., Khoo, B. L., Wu, L., Tay, A. K., et al. Ultra-fast, label-free isolation of circulating tumor cells from blood using spiral microfluidics. Nat. Protoc. 2016, 11, 134–148.
19. El-Heliebi, A., Kroneis, T., Zohrer, E., Haybaeck, J., et al. Are morphological criteria sufficient for the identification of circulating tumor cells in renal cancer?. J. Transl. Med. 2013, 11, 214.
20. Mu, Z., Benali-Furet, N., Uzan, G., Znaty, A., et al. Detection and characterization of circulating tumor associated cells in metastatic breast cancer. Int. J. Mol. Sci. 2016, 17, 1665.
21. Yusa, A., Toneri, M., Masuda, T., Ito, S., et al. Development of a new rapid isolation device for circulating tumor cells (CTCs) using 3D palladium filter and its application for genetic analysis. PLoS One 2014, 9, e88821.
22. Hosokawa, M., Hayata, T., Fukuda, Y., Arakaki, A., et al. Size-selective microcavity array for rapid and efficient detection of circulating tumor cells. Anal. Chem. 2010, 82, 6629–6635.
23. Hosokawa, M., Kenmotsu, H., Koh, Y., Yoshino, T., et al. Size-based isolation of circulating tumor cells in lung cancer patients using a microcavity array system. PLoS One 2013, 8, e67466.
24. Negishi, R., Hosokawa, M., Nakamura, S., Kanbara, H., et al. Development of the automated circulating tumor cell recovery system with microcavity array. Biosens. Bioelectron. 2015, 67, 438–442.
25. Hosokawa, M., Yoshikawa, T., Negishi, R., Yoshino, T., et al. Microcavity array system for size-based enrichment of circulating tumor cells from the blood of patients with small-cell lung cancer. Anal. Chem. 2013, 85, 5692–5698.
26. Yoshino, T., Tanaka, T., Nakamura, S., Negishi, R., et al. Manipulation of a single circulating tumor cell using visualization of hydrogel encapsulation toward single-cell whole-genome amplification. Anal. Chem. 2016, 88, 7230–7237.
27. Negishi, R., Takai, K., Tanaka, T., Matsunaga, T., et al. High-throughput manipulation of circulating tumor cells using a multiple single-cell encapsulation system with a digital micromirror device. Anal. Chem. 2018, 90, 9734–9741.
28. Negishi, R., Iwata, R., Tanaka, T., Kisailus, D., et al. Gel-based cell manipulation method for isolation and genotyping of single-adherent cells. Analyst 2019, 144, 990–996.
29. Schwanhausser, B., Busse, D., Li, N., Dittmar, G., et al. Global quantification of mammalian gene expression control. Nature 2011, 473, 337–342.
30. Lin, J., Jordi, C., Son, M., Van Phan, H., et al. Ultra-sensitive digital quantification of proteins and mRNA in single cells. Nat. Commun. 2019, 10, 3544.
31. Yagi, S., Koh, Y., Akamatsu, H., Kanai, K., et al. Development of an automated size-based filtration system for isolation of circulating tumor cells in lung cancer patients. PLoS One 2017, 12, e0179744.

SUPPORTING INFORMATION

Additional supporting information may be found online in the Supporting Information section at the end of the article.

How to cite this article: Negishi R, Saito H, Iwata R, Tanaka T, Yoshino T. Performance evaluation of a high-throughput separation system for circulating tumor cells based on microcavity array. *Eng Life Sci*. 2020;20:485–493. https://doi.org/10.1002/elsc.202000024